Young Neutron Stars and Their Environments
IAU Symposium, Vol. 218, 2004
F. Camilo and B. M. Gaensler, eds.

XMM-Newton and Geminga

Patrizia Caraveo, Andrea De Luca, Sandro Mereghetti, Alberto Pellizzoni

Istituto di Astrofisica Spaziale e Fisica Cosmica, Sezione di Milano "G.Occhialini" — CNR, Via Bassini 15, I-20133 Milano, Italy

Giovanni Bignami[1], Anatoly Tur

Centre d'Etude Spatiale des Rayonnements, Toulouse, France
and [1] *Università degli Studi di Pavia, Via Ugo Bassi, 6 — Pavia, Italy*

Roberto Mignani

European Southern Observatory, D-85740, Garching bei München, Germany

Werner Becker

Max-Plank Institut für Extraterrestrische Physik, 85741 Garching bei München, Germany

Abstract. A deep *XMM-Newton*/EPIC observation of the field of the Geminga pulsar unveiled the presence of two elongated parallel X-ray tails trailing the neutron star. They are aligned with the object's supersonic motion, extend for $\sim 2'$, and have a nonthermal spectrum produced by electron-synchrotron emission in the bow shock between the pulsar wind and the surrounding medium. Such a *first ever* X-ray detection of a pulsar bow shock allows us to gauge the pulsar electron injection energy and the shock magnetic field while constraining the angle of Geminga's motion and the local matter density.

1. Observing Geminga with EPIC

On 2002 Apr 4, *XMM-Newton* performed a 100 ksec observation of Geminga. During this observing time, the three cameras of the EPIC detector collected at once a harvest of photons equivalent to double of the photon database available for Geminga since it was discovered by the Einstein observatory. (Bignami, Caraveo & Lamb 1983). Thus, it comes as no surprise that our EPIC observation unveiled unseen details in Geminga's phenomenology adding yet again another first on the rich and lively source history (Bignami & Caraveo 1996).

Geminga's observation was performed with the two MOS cameras in "full frame" mode (Turner et al. 2001), and the pn camera in "small window" mode to allow for accurate timing of source photons (Strüder et al. 2001). Data were processed with the *XMM-Newton* Science Analysis Software (SAS version 5.4.1).

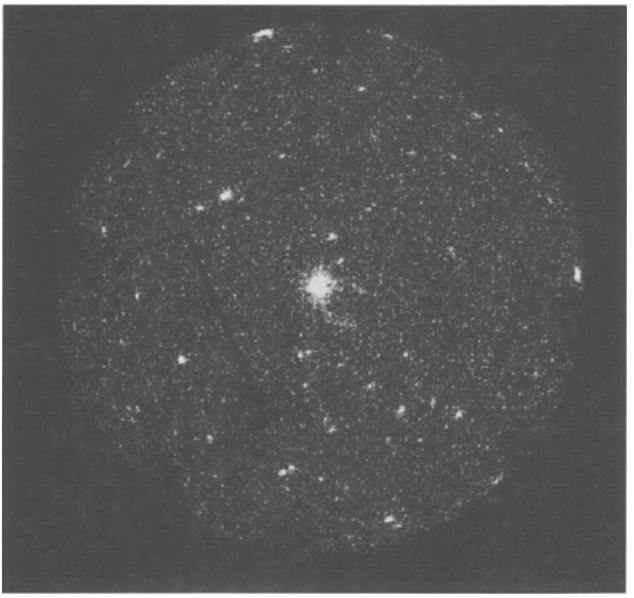

Figure 1. The *XMM-Newton* view of the field of Geminga ($0.3 < E < 5$ keV). Data from the MOS1 and MOS2 $\sim$ 77 ksec exposures have been merged to produce the image. Geminga is the bright source close to the center of the image; the tails can be seen as two faint diffuse emission patterns emerging from the source. Many ($\sim$ 100) serendipitous sources are also visible in the field.

After removing time intervals with high particle background and correcting for the dead time, we obtain a net exposure time of 55.0 ksec for the pn camera and 76.9 and 77.4 ksec for the MOS1 and MOS2, respectively. The Geminga count rates ($0.2 < E < 7$ keV) are 0.807 ± 0.004 counts s^{-1} for the pn and 0.119 ± 0.001 counts s^{-1} and 0.123 ± 0.001 counts s^{-1} for the MOS1 and MOS2, respectively.

2. Imaging Geminga with EPIC

The sum of the MOS1 and MOS2 images is shown in Figure 1. Besides Geminga, which shines at the center of the image, more than 100 serendipitous sources have been detected. Identification work is in progress on such sources and will be reported elsewhere. For a thorough discussion of the "tails", which are seen by EPIC for the first time trailing Geminga and well aligned with the source proper motion (see Fig. 2 left), the reader is referred to Caraveo et al. (2003). Here, we point out the most important characteristics of this newly-discovered, and so far unique, X-ray feature of Geminga.

The tails are two patterns of diffuse emission, originating close to Geminga (they cannot be resolved in proximity of the bright point source to closer than $40''$) and extending up to $\sim 3'$ away from the pulsar, well aligned with the neutron star proper motion, with a thickness of $\sim 20''$–$30''$. Their spectrum is

https://doi.org/10.1017/S007418090018101X Published online by Cambridge University Press

well reproduced by a slightly absorbed ($N_H \sim 10^{20}\mathrm{cm}^{-2}$) power law with photon index $\Gamma \sim 1.6$. At the pulsar distance (160 pc), their unabsorbed 0.3–5 keV flux corresponds to a luminosity of 6.5×10^{28} ergs s^{-1} ($\sim 2 \times 10^{-6}$ of Geminga's rotational energy loss). Possible contributions from point sources are estimated to be negligible.

The shape of the tails is reminiscent of the projection on the plane of the sky of an empty paraboloid of X-ray emission, the edges of which show up brighter because of a limb effect. Such a morphology is naturally explained in terms of a bow-shock formed between the pulsar relativistic wind and the dynamical pressure generated by its supersonic motion through the interstellar medium. The observed geometry of the tails, compared to a 3-D bow-shock model assuming a spherical pulsar wind in an homogeneous ISM, allows also to constrain the angle of the source motion with respect to the plane of the sky to be less than $\sim 30°$, and therefore to assess its 3-D space velocity. The detection of the pulsar bow-shock represents also an important way to probe the interstellar medium, constraining its density to be in the range 0.06–0.15 atoms cm^{-3}, in good agreement with the expected value of the ISM density for the region around Geminga (Gehrels & Chen 1993).

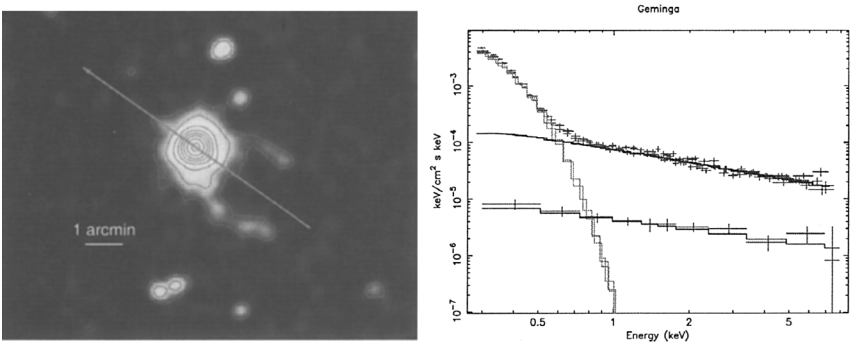

Figure 2. *Left panel:* Inner part of the field of Figure 1, shown after gaussian smoothing. The emission from Geminga outshines the tails up to $\sim 40''$ from the source. The tails are $\sim 2'$ long and cover an area of $\sim$2 square arcmin. They show a remarkable symmetry with respect to the pulsar proper motion direction, marked by the arrow. *Right panel:* Unfolded spectrum of Geminga (upper curve) superimposed on the tails' (lower curve).

3. EPIC Spectral Studies

The good EPIC statistics allow for an accurate spectrum to be drawn, for the first time, of both the pulsar and its tails, in the range 0.2 to $\sim$7 keV. Figure 2 (right) shows such a time-averaged spectrum for both the pulsar (upper curve) and its surrounding diffuse emission (lower curve). Note that the upper curve plots both the pn and the two MOS data sets (superimposed and indistinguishable), while the lower curve for the extended emission (tails) contains

https://doi.org/10.1017/S007418090018101X Published online by Cambridge University Press

MOS data only, since the pn camera was used in "small window" mode. While a more detailed interpretation of the source physics as portrayed by Figure 2 (right) will be the topic of upcoming work, we propose here a few qualitative, obvious comments. The point-source spectrum (upper curve) shows with a striking clarity that two different mechanisms are at work. Below $\sim$ 0.7 keV, the emission is undoubtedly thermal, well fit by a black-body with temperature of $\sim$43 eV, implying an emitting surface of $\sim$ 9 km at the parallax distance of 160 parsec (Caraveo et al. 1996). For the whole energy decade 0.7–7 keV, a power law, with photon index $\Gamma \sim 1.85$, dominates Geminga's spectrum. The simplest interpretation of such a hard power law, already seen when combining the *ROSAT* and *ASCA* data sets (Jackson et al. 2002), is that of synchrotron emission by energetic electrons radiating in the pulsar magnetic field.

For the diffuse emission from the tails (lower curve of Fig. 2, right panel), a best-fitting power law index of $\sim$ 1.6 points to a striking similarity with the hard spectral shape of the point source. This points to a similar physical origin between the point source and the tails' hard X-ray photons. Indeed, the spectrum of the tails can be explained by synchrotron emission of high-energy electrons accelerated by the pulsar, gyrating in the shocked interstellar magnetic field of $\sim 10\,\mu$G (see Caraveo et al. 2003 for a complete discussion). Such an interpretation provides a direct gauge of the pulsar wind injection energy, demonstrating that Geminga accelerates electrons up to 10^{14} eV, a value very close to the upper limits expected on the basis of the pulsar's energetics, allowing also to constrain the local interstellar magnetic field to the range 2–3 μG. The Larmor radius of the emitting electrons in the bow-shock magnetic field ($\sim 27''$ at the distance of Geminga) is found to be in excellent agreement with the observed thickness of the tails. Moreover, the electron lifetime against synchrotron emission ($\sim$ 800 years) matches the pulsar transit time over the X-ray length of the features ($\sim$ 1000 years, on the basis of the well known proper motion of Geminga), supplying a final, independent consistency check to our model.

References

Bignami, G. F., Caraveo, P. A., & Lamb, R. C. 1983, ApJ, 272, L9

Bignami, G. F., & Caraveo, P. A. 1996, ARA&A, 34, 331

Caraveo, P. A., Bignami, G. F., Mignani, R., & Taff, L. G. 1996, ApJ, 461, L91

Caraveo, P. A., Bignami, G. F., DeLuca, A., Mereghetti, S., Pellizzoni, A., Mignani, R., Tur, A., & Becker, W. 2003, Science, 301, 1345

Gehrels, N., & Chen, W. 1993, Nature, 361, 706

Jackson, M. S., Halpern, J. P., Gotthelf, E. V., & Mattox, J. R. 2002, ApJ, 578, 935

Strüder, L., et al. 2001, A&A, 365, L18

Turner, M. J. L., et al. 2001, A&A, 365, L27